

RESEARCH ARTICLE | JULY 07 2010

Long-wavelength optical transmission of extremely narrow slits via hybrid surface-plasmon and Fabry–Pérot modes

X. F. Li; S. F. Yu



J. Appl. Phys. 108, 013302 (2010)

<https://doi.org/10.1063/1.3457841>



Articles You May Be Interested In

The resonant electromagnetic fields of an array of metallic slits acting as Fabry–Pérot cavities

J. Appl. Phys. (June 2006)

Ultra-narrow electromagnetically induced transparency in the visible and near-infrared regions

Appl. Phys. Lett. (May 2019)

Angle insensitive filters based on Fabry–Pérot resonance structures

J. Appl. Phys. (November 2024)



Journal of Applied Physics

Special Topics Open for Submissions

[Learn More](#)

Long-wavelength optical transmission of extremely narrow slits via hybrid surface-plasmon and Fabry–Pérot modes

X. F. Li and S. F. Yu^{a)}*School of Electrical and Electronic Engineering, Nanyang Technological University, Singapore 639798*

(Received 15 February 2010; accepted 1 June 2010; published online 7 July 2010)

We have verified that extraordinary transmission of long-wavelength light through extremely narrow slits in a thick metal film can be achieved by hybrid surface-plasmon and Fabry–Pérot modes. Transmittance of these ultranarrow slits, which have width and thickness of $0.56\ \mu\text{m}$ and $100\ \mu\text{m}$, respectively, for a terahertz light with wavelength of $225\ \mu\text{m}$ can be 2.1×10^8 times higher than that predicted by using classic theory. Furthermore, the corresponding ratio between transmission wavelength and slit width can be up to 400, which is over 60 times larger than that the conventional grating-based surface-plasmon modes can provide. © 2010 American Institute of Physics. [doi:10.1063/1.3457841]

I. INTRODUCTION

Extraordinary optical transmission (EOT) through sub-wavelength aperture has attracted tremendous attention since the first study reported by Ebbesen *et al.*¹ a decade ago. It is widely believed that the EOT is mainly attributed to the excitation of surface plasmons (SPs) on a periodically perforated metal surface.^{2–4} On the other hand, there was evidence explaining that the contribution of strong light transmission might be related to Wood–Rayleigh anomalies.^{5,6} Nevertheless, the allowed longest value of the resonant wavelength for EOT, which is mainly based on grating-defined SPs, was observed only slightly larger than the grating period.⁷ Hence, in order to maintain the amount of transmittance, the ratio between transmission wavelength and aperture size has to be limited to a small value (i.e., the aperture cannot be too narrow and the transmission wavelength cannot be too long).

In the previous studies of EOT phenomenon, longitudinal Fabry–Pérot (FP) modes can be formed inside the periodic metal slits if the metal thickness is large enough so that strong transmission of light can be achieved.^{2–4,8,9} However, little attention has been paid to the transmission capability of these cavity modes, which transmittance can be even higher than that of the SPs.³ Most importantly, the wavelengths of these modes are mainly dependent on the longitudinal resonant conditions and are independent of the grating period.⁵ This indicates that ultranarrow slits can allow light with a very long wavelength to travel through.

The aim of this paper is to study the mechanism of EOT in periodic deep-subwavelength slits via the excitation of longitudinal FP modes. The underlying physics of this type of modes is revealed by using finite-difference time-domain (FDTD) technique and rigorous coupled-wave model (RCWM).^{10–13} It is found that the EOT in long wavelengths is originated from the combined effect of longitudinal SPs (LSPs) and FP modes under transverse-magnetic (TM) incidence. It is noted that 20% transmittance for a terahertz light at wavelength of $225\ \mu\text{m}$ can be obtained through narrow

slits with width and thickness of $0.56\ \mu\text{m}$ and $100\ \mu\text{m}$, respectively. The transmittance is 2.1×10^8 times higher than the prediction of Bethe's theory.^{14,15} Moreover, the corresponding wavelength-aperture ratio is over 60 times larger than that the metallic grating defined SPs can realize.

II. DEVICE STRUCTURE AND DRUDE MODEL

Schematic of a one-dimensional metallic grating used for this study of the longitudinal FP modal transmission is displayed in Fig. 1, where d is the thickness of the Au film surrounded by vacuum, w is the slit width, θ is the incident angle, and the grating period Λ is fixed at $3.5\ \mu\text{m}$. Only normal incidence (i.e., $\theta=0^\circ$) is considered in the analysis because dispersion characteristics of the longitudinal FP modes are almost independent on θ .³ This large-index-contrast metallic grating can be modeled by using RCWM with which a large number of spatially harmonic components can be taken into consideration.¹² Full-vectorial FDTD calculation will also be performed for a comprehensive investigation of EOT.¹⁰ In the calculation, the permittivity of Au is modeled by the modified Drude formula¹⁶

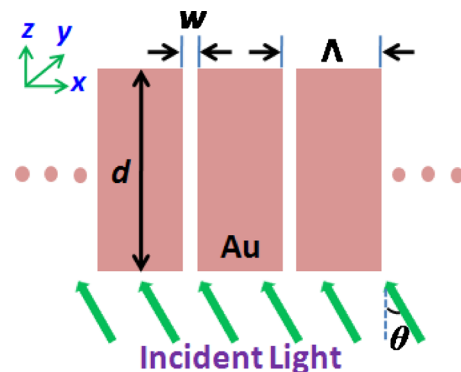


FIG. 1. (Color online) Schematic of the structure under consideration for long-wavelength EOT using periodic deep-subwavelength slits.

^{a)}Present address: Department of Applied Physics, The Hong Kong Polytechnic University, Hung Hom, Kowloon, Hong Kong.

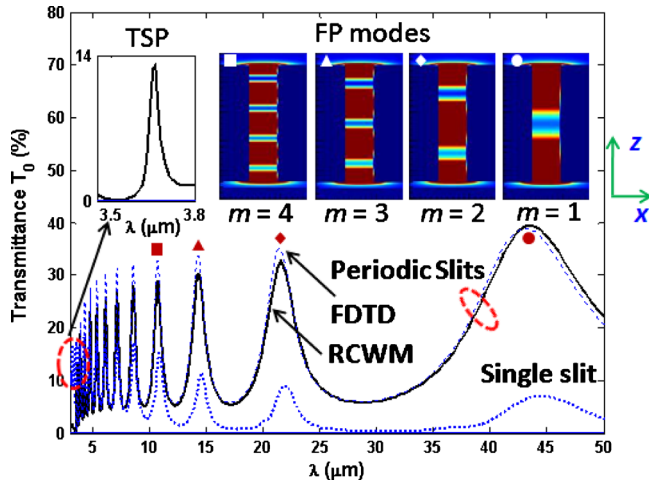


FIG. 2. (Color online) Transmission spectra of a thick Au film ($d = 20 \mu\text{m}$) with periodic slits ($\Lambda = 3.5 \mu\text{m}$, $w = 0.5 \mu\text{m}$) and a stand-alone slit ($w = 0.5 \mu\text{m}$). The xz images of field intensities of FP modes with $m = 1-4$ are inserted, where only one period of the grating is displayed. The enlarged reflection spectrum at $\lambda \sim \lambda_{sp}$ is also inserted.

$$\varepsilon_M = \varepsilon_\infty - \frac{\omega_p^2}{\omega^2 + i\gamma\omega} + \varepsilon_{x1} + \varepsilon_{x2}, \quad (1)$$

where ε_∞ is the permittivity under high-frequency limit, ω_p is the bulk plasma frequency, γ is the electron decaying rate, and ε_{x1} and ε_{x2} are the contributions of interband transitions. The parameters used in this model are taken from Ref. 16.

III. TRANSMISSION SPECTRUM

In order to realize long-wavelength EOT, the thickness of the Au film, d , is set to $20 \mu\text{m}$ for the excitations of long-wavelength FP modes. Figure 2 plots the transmission spectrum of the periodic slits with $w = 0.5 \mu\text{m}$, where the incident electric field is assumed linearly polarized along the x direction (i.e., TM incidence). The solid and dashed lines represent the calculation of EOT of the periodic slits via RCWM (which has taken over 100 diffraction waves into calculation)¹³ and FDTD techniques. It is observed that both techniques give similar results except that there are slightly different in the magnitude of peak transmittances, T_0 . As shown in Fig. 2, a series of resonant peaks at wavelength λ_{pm} , where $m = 1, 2, \dots, \infty$ is the order of longitudinal FP modes, is excited from the periodic slits. T_0 of the four lowest-order FP modes at wavelength of $43.11 \mu\text{m}$, $21.41 \mu\text{m}$, $14.24 \mu\text{m}$, and $10.69 \mu\text{m}$ are found to be 28.73%, 27.91%, 26.84%, and 25.82% respectively. The FP wavelengths can be estimated according to the cavity resonant condition $k \text{Re}(n_{\text{eff}})d + \Delta\Phi = m\pi$, where n_{eff} is the effective refractive index of the corresponding metal-dielectric-metal (MDM) cavity, and $\Delta\Phi$ is the phase change due to the reflection of the FP facet. The electric field profiles of the four lowest-order FP modes calculated by FDTD method are also shown in the insets of Fig. 2.

Nevertheless, a peak value of T_0 at wavelength λ equals to $3.64 \mu\text{m}$ (i.e., see the inset of Fig. 2) corresponds to a SP mode defined by the grating along the transverse direction (i.e., x direction). We therefore define this type of modes as the transverse SP (TSP) mode in the following paragraphs of

wavelength λ_{sp} . TSP mode can be excited under the *transverse phase-matching condition* (PMC):⁷

$$\text{Re}(\beta_{sp-T}) = k \sin \theta \pm n \frac{2\pi}{\Lambda}, \quad (2)$$

where $\beta_{sp-T} = k\sqrt{\varepsilon_M/(1+\varepsilon_M)}$ is the propagation constant of the TSP mode confined by the metal-dielectric (MD) interface, $k = 2\pi/\lambda$, and $n = 1, 2, \dots, \infty$ is the diffraction order. It is found that the value of λ_{sp} obtained from both RCWM and FDTD calculations is slightly red-shifted from that predicted by Eq. (2).¹⁵ It is noted that the value of T_0 at λ_{sp} is just 13.1%, which is less than 50% to that of the FP modes can obtain. Moreover, the value of λ_{sp} is over tens of times less than that of λ_{p1} . These revealed that the transmission performance of the FP modes excited from the thick metal film for both values of T_0 and λ can be significantly larger than that of the conventional TSP modes.^{3,5}

Figure 2 also plots the variation of T_0 versus λ of a stand-alone slit (dotted line).^{17,18} Although the transmission is less efficient than that of the periodic system due to the lack of interactions between the light from different slits, the transmittance observed from the single slit is still larger than that the normal FP modes (i.e., without SP feature) in sub-wavelength slits can provide. This implies that that the longitudinal resonance of FP modes is not the only mechanism contributing to the EOT through the deep-subwavelength slits at long wavelength. Using FDTD technique, we recalculated the transmission spectrum of the single slit under a transverse-electric incidence. In this case, SPs will not be excited and T_0 was found to be extremely low (in order of 10^{-12}) at all wavelengths. It is therefore postulated that the LSPs excited inside the metal slit (i.e., LSP modes) should be responsible for the EOT in conjunction with the FP modes. We thus define this type of modes as the hybrid LSP-FP modes, which can be excited when the *longitudinal PMC* is fulfilled

$$\text{Re}(\beta_{sp-L}) = k \cos \theta \pm m \frac{2\pi}{d}, \quad (3)$$

where β_{sp-L} is the propagation constant of the LSPs supported by a MDM waveguide. The value of β_{sp-L} can be estimated by using transfer-matrix method.¹⁹ It is obvious that the resonant conditions of these hybrid modes are mainly dependent on the value of d . It is also noted in Fig. 2 that the values of λ_{pm} are identical for the cases with periodic and stand-alone slit so that Eq. (3) should be independent of Λ .

IV. HYBRID FEATURES OF THE TRANSMITTED MODES

The hybrid feature can be observed from Fig. 3, which plots the electric field profiles of the fundamental and second-order LSP-FP modes along the x and z directions, respectively. The slit with MDM structure along x direction is responsible for the formation of symmetric SP modes,⁷ while the formation of standing cavity wave under the frequency selectivity in z direction determines the transmission wavelength. Furthermore, the peak intensities appear at the

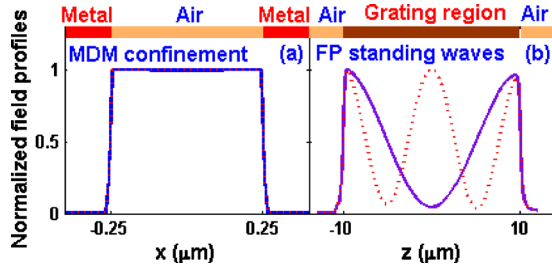


FIG. 3. (Color online) Modal profiles along x (only one period is displayed) and z directions of LSP-FP modes with $m=1$ (solid) and $m=2$ (dotted), calculated using FDTD technique.

dielectric-metal interfaces along the x and z directions. These verified that the total field transmitted through the metal slit is consisted of SP and FP components along the x and z directions, respectively.

Figure 4(a) and 4(b) show the profile of electric fields at $\lambda=\lambda_{sp}$ (i.e., the TSP mode in Fig. 2) and λ_{p1} (i.e., the fundamental LSP-FP mode in Fig. 2), respectively, inside the periodic slits with a perfectly-matched layer (PML) applied to the top surface of the structure in order to avoid optical feedback.²⁰ It is observed that the intensity of the modes at both wavelengths is weakened due to the lack of optical feedback. However, the TSP mode can still be excited at $\lambda=\lambda_{sp}$, while no FP feature is established at $\lambda=\lambda_{p1}$. This shows that the formation of FP properties of the LSP-FP modes is due to the optical feedback at the top and bottom surfaces of the slits. However, there is no physical facet presented at the top and bottom surfaces providing optical feedback. In fact, optical feedback may be attributed to the unique confining capability of SPs. Light confined within the metal part may experience a very large discontinuity in refractive index at the top and bottom surfaces of the metal region so that strong optical feedback can be achieved.

V. STRONG SELF-FEEDBACK OF MDM STRUCTURE

To further examine the resonant characteristics of the LSP-FP hybrid modes, the transmission characteristics of a modified nonuniform periodic configuration are investigated, see Fig. 5(a) for one period of the metal-slit schematic. Figure 5(b) plots T_0 versus λ of the nonuniform periodic metal-slit (solid line). The transmission spectrum of the uniform periodic metal-slit with film thickness of $20\ \mu\text{m}$ (i.e., dot

line, the same to that considered in Fig. 2) is also shown in the figure for comparison. It is observed that although the introduced MD section slightly perturbs the transmission spectrum through the optical feedback from the upper interface, the FP resonance is mainly determined by the MDM section. In addition, the MD section has minimum influence on the FP resonant condition of the metal slits. The corresponding field profile of the fundamental LSP-FP mode shown in Fig. 5(a) also verified that the MDM section dominates the FP resonant characteristics of the nonuniformly configured periodic slits. This is because light confined inside the MDM section is stronger than that in MD structure⁷ so that more light is resided in the metal regions of MDM section and therefore contributes stronger optical feedback.

VI. DEVICE OPTIMIZATION

It is interesting to design the dimensions of the ultranarrow metal slits with the optimized value of T_0 . This is required to maximize the values of wavelength-aperture ratio (i.e., λ_{pm}/w) and T_0 for a given d simultaneously. This can be done by searching for the largest value of $T_0 \lambda_{pm}/w$. Figure 6(a) depicts the dependences of T_0 and $T_0 \lambda_{pm}/w$ on w with d set to $20\ \mu\text{m}$. The lowest four order LSP-FP modes are discussed in this study [also in Fig. 6(b)]. It is observed that there is an optimal value of w (i.e., $\sim 0.56\ \mu\text{m}$) for the largest $T_0 \lambda_{pm}/w$. Using this value, we then focus on the design of d in Fig. 6(b). It is shown that a maximal T_0 can be achieved at $d \sim 1.4\ \mu\text{m}$; however, the value of $T_0 \lambda_{pm}/w$ is too small. The value of $T_0 \lambda_{pm}/w$ can be improved by increasing the value of d but the increase in d also degrades the value of T_0 . Therefore, the proper design should also subject to a desired transmittance. As shown in Fig. 6(b), if using an Au film with thickness of $50\ \mu\text{m}$ ($100\ \mu\text{m}$), T_0 for the light at $109\ \mu\text{m}$ ($225\ \mu\text{m}$) can be 28.4% (18.6%) for the first-order LSP-FP mode.

Bethe's theory can be used to roughly estimate the value of T_0 of the periodic slits. Despite it is used to calculate the transmittance from a subwavelength hole (i.e., $T_0 = 64(kr)^4/27\pi^2$, where k is the light wave number and r is the hole radius),¹⁴ the calculated result should be compatible for the slit structure. This is because the TM modes are polarized perpendicular to the homogenous direction (i.e., y direction, see Fig. 1). For the metal slit with $w \sim 0.56\ \mu\text{m}$, the calculated values of T_0 for light with wavelength of 109

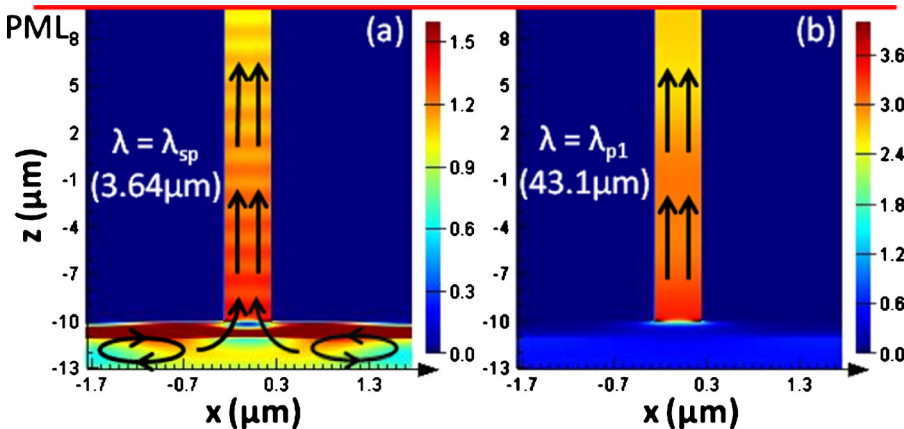


FIG. 4. (Color online) Field distributions of the modes at λ_{sp} (a) and λ_{p1} (b) in xz plane where a PML is applied to the upper grating interface. Here, only one period of the grating is displayed.

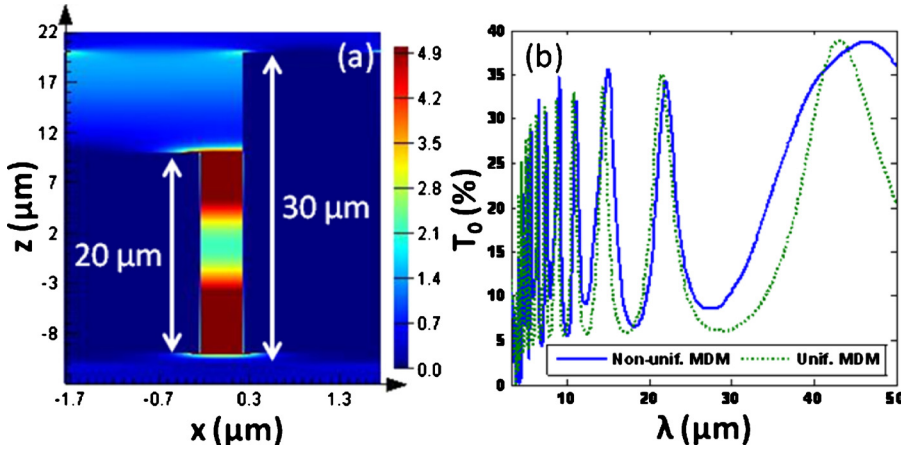


FIG. 5. (Color online) (a) Field distribution of first-order LSP-FP mode in xz plane, where the metal thickness on the right-side of each slit is increased to $30 \mu\text{m}$ (i.e., nonuniform periodic MDM structure). The resonant wavelength used in Fig. 5(a) is taken from the corresponding transmission spectrum (b) calculated by FDTD method, where the result of uniform periodic MDM structure is also inserted (dot curve). Here, only one period of the grating is displayed.

and $225 \mu\text{m}$ are found to be 8.98×10^{-10} and 1.63×10^{-8} , respectively. Our designed transmittances shown in Fig. 6 are therefore 2.1×10^8 and 1.7×10^7 times higher than those expected through this classic theory. T_0 at TSP wavelength is also calculated using this formula and is found to be only $\sim 1/10$ of that obtained in this simulation. Moreover, the λ_{p1}/w ratio using LSP-FP modes for EOT can be over 60 times of that based on TSP mode (i.e., $225/3.5 \sim 64$) and a higher transmittance can be obtained (as discussed previously, T_0 based on TSP is only 13.1% even with a thinner film, i.e., $20 \mu\text{m}$). Hence, we indicated that the high transmittance through such a thick metal film is also due to the fact that the SP loss in the MDM structure is actually decreased with the increase in the wavelength. This can be easily confirmed by employing transfer-matrix calculation.

It should also be pointed out that the transmission wavelength (λ_{p1}) and the dimensions of metal slits (d, w, Λ) can be “approximately” scaled up or down for the EOT applications. We said approximately because the permittivity of Gold is not scalable with the transmission wavelength. In Fig. 7, three transmittance spectra are plotted, where the scaling ratios in (a), (b), and (c) are taken to be 0.1, 1, and 10, respectively. This implies that the values of d, w , and Λ are

obtained by multiplying the optimized configurations of the metal slits given in Fig. 6(b) (i.e., $d=50 \mu\text{m}$, $w=0.56 \mu\text{m}$, $\Lambda=3.5 \mu\text{m}$) to 0.1, 1.0 and 10. It is observed that the peak transmission wavelength and the dimension of metal slits show rough proportion to the scaling ratio. In Figs. 7(a)–7(c), the values of λ_{p1} (scaling ratio) are found to $\sim 10.9(0.1)$, $\sim 109(1.0)$, and $\sim 1090 \mu\text{m}$ (10), respectively. See also the red dots in Fig. 7 where the value of transmittance is maximized. Therefore, it is verified that high-transmission of narrow metal slits can be achieved in a very broad frequency range.

VII. CONCLUSION

In summary, it is found that the formation of hybrid LSP-FP modes is the origin of long-wavelength EOT through extremely narrow slits. This type of modes, which shows significantly improved transmission capability through extremely narrow slits, is fundamentally different from the conventional SPs defined by the periodic slits. For periodic slits with width and thickness equal to 0.56 and $100 \mu\text{m}$, it is found that the transmittance can be over 2

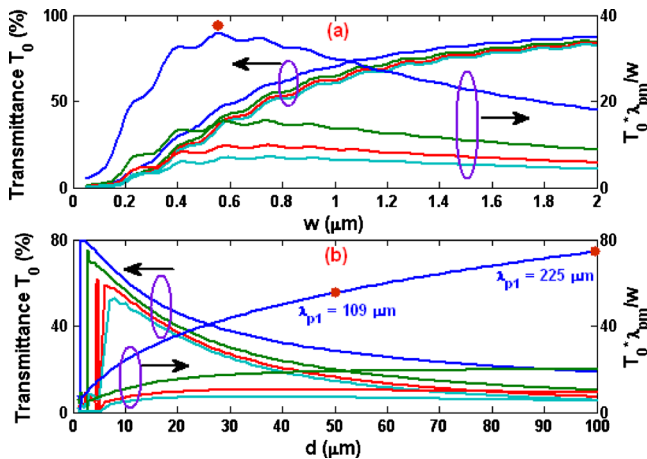


FIG. 6. (Color online) Effects of w (a) and d (b) on the transmission and FP resonant characteristics of the structure, where $m=1$ (solid), 2 (dashed), 3 (dotted), and 4 (dashed-dotted). (a): $d=20 \mu\text{m}$, where maximal value of T_0 λ_{p1}/w occurs at $w=0.56 \mu\text{m}$ and (b): $w=0.56 \mu\text{m}$. The results are calculated through RCWM.

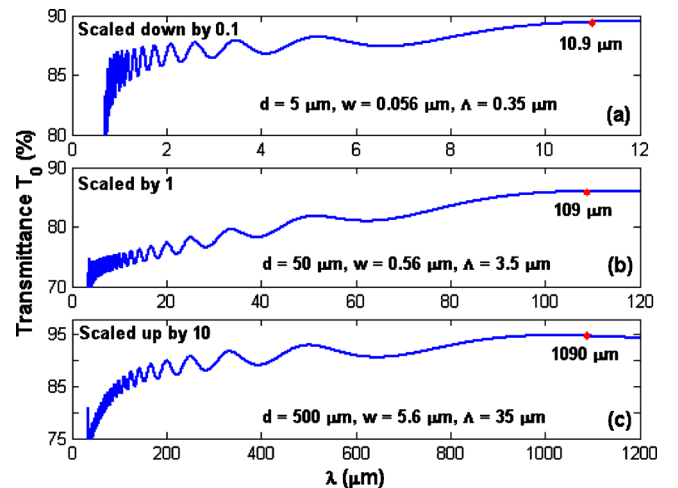


FIG. 7. (Color online) Transmittance spectra after optimization. The scaling ratio of the metal slits is set to (a) 0.1, (b) 1.0, and (c) 10. RCWM is used for this calculation.

$\times 10^8$ times of that predicted from Bethe's theory and the wavelength can be as long as $225\ \mu\text{m}$ (i.e., the slit width is only 1/400 of the transmitted wavelength).

ACKNOWLEDGMENTS

This work is supported by the A*STAR SERC grant under Grant No. 082-101-0016.

- ¹T. W. Ebbesen, H. J. Lezec, H. F. Ghaemi, T. Thio, and P. A. Wolff, *Nature (London)* **391**, 667 (1998).
- ²H. F. Ghaemi, T. Thio, D. E. Grupp, T. W. Ebbesen, and H. J. Lezec, *Phys. Rev. B* **58**, 6779 (1998).
- ³J. A. Porto, F. J. García-Vidal, and J. B. Pendry, *Phys. Rev. Lett.* **83**, 2845 (1999).
- ⁴Z. C. Ruan and M. Qiu, *Phys. Rev. Lett.* **96**, 233901 (2006).
- ⁵Q. Cao and P. Lalanne, *Phys. Rev. Lett.* **88**, 057403 (2002).
- ⁶D. Crouse and P. Keshavareddy, *Opt. Express* **13**, 7760 (2005).
- ⁷S. A. Maier, *Plasmonics: Fundamentals and Applications* (Springer, New York, 2007).
- ⁸F. Marquier, J. J. Greffet, S. Collin, F. Pardo, and J. L. Pelouard, *Opt. Express* **13**, 70 (2005).
- ⁹J. Lindberg, K. Lindfors, T. Setälä, M. Kaivola, and A. T. Friberg, *Opt. Express* **12**, 623 (2004).
- ¹⁰FDTD Solutions, <http://www.lumerical.com/>
- ¹¹X. F. Li, S. F. Yu, and A. Kumar, *Appl. Phys. Lett.* **95**, 141114 (2009).
- ¹²M. G. Moharam, D. A. Pommet, E. B. Grann, and T. K. Gaylord, *J. Opt. Soc. Am. A* **12**, 1077 (1995).
- ¹³X. F. Li and S. F. Yu, *J. Appl. Phys.* **106**, 053103 (2009).
- ¹⁴H. A. Bethe, *Phys. Rev.* **66**, 163 (1944).
- ¹⁵C. Genet and T. W. Ebbesen, *Nature (London)* **445**, 39 (2007).
- ¹⁶P. G. Etchegoin, E. C. Le Ru, and M. Meyer, *J. Chem. Phys.* **125**, 164705 (2006).
- ¹⁷Y. Takakura, *Phys. Rev. Lett.* **86**, 5601 (2001).
- ¹⁸J. R. Suckling, A. P. Hibbins, M. J. Lockyear, T. W. Preist, and J. R. Sambles, *Phys. Rev. Lett.* **92**, 147401 (2004).
- ¹⁹M. Born and E. Wolf, *Principles of Optics: Electromagnetic Theory of Propagation, Interference and Diffraction of Light* (Pergamon, Oxford, 1964).
- ²⁰W. P. Huang, C. L. Xu, W. Lui, and K. Yokoyama, *IEEE Photonics Technol. Lett.* **8**, 652 (1996).